

STRUCTURAL STUDY OF Fe-Mn-Si AND Fe-Mn-Cr SHAPE MEMORY STEELS

K. TAMARAT, V. STAMBOULI, T. BOURAOUI and B. DUBOIS

ENSCP, Applied Metallurgy, 11 rue P. et M. Curie, F-75231 Paris cedex 05, France

Abstract - In Fe-Mn-Si and Fe-Mn-Cr steels, γ and ϵ phases, which give rise to shape memory effect, were observed at room temperature. In order to determine the transition temperatures, different methods were carried out. Depending on the method, the results were different. The transition temperatures either appeared or were not found in the studied temperature range. It was thought of developing a stress induced martensite to improved the results, particularly those obtained by X ray diffraction experiments.

INTRODUCTION

It is well known that Fe-Mn-Si shape memory steels do not resist to corrosion (1). In Fe-Mn-Cr, the partial shape memory could disappear by wrong thermomechanical treatments. However, it would be interesting to study some of these alloys in order to understand the shape memory effect in steels.

After structural characterization at room temperature, we looked for methods and conditions to determine the transition temperatures.

EXPERIMENTAL

Two Fe-Mn-Si alloys were swaged to 18 x 18 mm² bar and water quenched. The chemical compositions were the following (in wt %):

- S₁ (Mn : 31.6 - Si : 6.45 - C : 0.018 - N : 0.0052 - S : 0.0079)
- S₂ (Mn : 26 - Si : 5 - Mo : 2 - Al < 0.8 - C < 0.01).

After melting and casting, two Fe-Mn-Cr alloys were homogenized during 48 hours at 1100°C, then hot rolled at 900°C before water quenching (thickness 10 mm).

The results of the chemical analysis were (in wt %) :

- C₁ (Mn : 14.13 - Cr : 12.36 - Al : 0.003 - Ni : 0.005 - Si : 0.03 - C : 0.019 - N : 0.0072 - O : 0.013)
- C₂ (Mn : 20.72 - Cr : 12.12 - Al : 0.003 - Ni : 0.005 - Si : 0.04 - C : 0.009 - N : 0.1724 - O : 0.010).

First of all, the structure of each alloy was studied on samples cut from the "as received" bars (S₁, S₂) or plates (C₁, C₂). Then, samples were maintained 1 hour at 1100°C before quenching in iced water and then soaked in liquid nitrogen. After electropolishing (10 % HClO₄ - 90 % butylcellosolve) and etching (SCHRÖDER reagent), the microstructure was observed by optical microscopy (Olympus). Electron microscopy experiments were performed on the Philips E.M. 300 apparatus. The preparation samples of Fe-Mn-Si was more difficult than those of the Fe-Mn-Cr specimens. X ray diffraction was carried out with Philips PW 1390 generator. After being polished, the shape memory effect was tested by bending at room temperature and heating at 300°C of thin specimens (0.2 mm - 0.7 mm). Electrical resistivity and internal friction (f = 1 Hz) measurements were also used to obtain the transformation temperatures.

RESULTS

After taking the necessary precautions of cleanliness and flatness of the surfaces, all the samples were studied at room temperature by microscopy and X ray diffraction ; the presence of γ austenite and ϵ martensite phases was noted. The body centred cubic structure α' was detected in the ferromagnetic C₁ alloy due to the low manganese content. However the b.c.c. structure was also observed in the S₂ alloy.

Then, for 0.2 to 0.7 mm thick samples the shape memory effect was observed. The best result was obtained during the heating of a S₁ sample (shape recovery of about 80 %) and this effect is really noticeable for the ferromagnetic C₁ alloy.

1. Structures at room temperature

1.1. Alloys S₁ and S₂ (Fe-Mn-Si)

The microstructure of the S₁ alloy is presented in fig. 1. Stacking faults and dislocations were observed by T.E.M. (fig. 2).

If a spark machined specimen (18 x 18 mm²) of the S₁ alloy was left at the temperature and humidity of the laboratory, X ray diffraction detects (111) _{γ} , (110) _{α'} , (200) _{γ} and other compounds partially crystallized. This means that oxidation produces the disappearance of the ϵ martensite, as noted by the absence of (10 $\bar{1}$ 0) and (10 $\bar{1}$ 1) lines. Microanalysis and I.R. spectroscopy showed roughly two oxide layers, the underlayer being enriched in manganese. After removing the oxide layers (about 100 μ m), ϵ and γ lines were detected. Furthermore, the removal of 600 μ m from the clean sample leads to a decrease in the ϵ line intensities.

The appearance of ϵ martensite depends on oxidation, manganese distribution and other parameters. From X ray diffraction for the S_1 alloy :

$$a_\gamma = 0.359 \text{ nm}, a_\epsilon = 0.253 \text{ nm}, c_\epsilon = 0.414 \text{ nm}, \frac{c}{a} = 1.636$$

In the case of the S_2 alloy :

$$a_\gamma = 0.361 \text{ nm}, a_\epsilon = 0.255 \text{ nm}, c_\epsilon = 0.416 \text{ nm}, \frac{c}{a} = 1.631 \text{ and } a_{\alpha'} = 0.287 \text{ nm.}$$

1.2. Alloys C_1 and C_2 (Fe-Mn-Cr)

The shape recovery is about 50 % for the C_2 alloy, nevertheless this effect can still be observed four years after training. It appears thus to have a good resistance to ageing. The microstructure is close to that of Fe-Mn-Si (fig. 3). Due to the chromium content, the oxidation phenomena were reduced even during heating.

The x ray diffraction spectrums are similar to those obtained with Fe-Mn-Si alloys. The lattice parameters of the C_2 alloy are :

$$a_\gamma = 0.360 \text{ nm}, a_\epsilon = 0.254 \text{ nm}, c_\epsilon = 0.415 \text{ nm}, c/a = 1.634.$$

The alloy C_1 is ferromagnetic with a small shape memory (very close to a Fe - 22 wt % Mn - 12 wt % Cr). It is not easy to detect α' martensite by optical micrography (fig. 4). From X ray diffraction, $(110)_{\alpha'}$ yields $a_{\alpha'} = 0.286 \text{ n.m.}$

At this stage of the study, we looked for the transformation temperatures according to the experimental conditions.

2. An approach of transformation temperatures of the studied alloys

Different methods were used to determine the transformation temperatures. In this work, cycling was not particularly studied. We noted that γ and ϵ phases were always detected by X ray diffraction at room temperature.

2.1. Alloys S_1 and S_2 (Fe-Mn-Si)

After maintaining 1 hour at 1100°C under an argon atmosphere, a S_1 sample ($e = 0.5 \text{ mm}$) was quenched in iced water and then soaked in liquid nitrogen. The specimen, carefully electropolished, was heated from room temperature up to 250°C while X ray diffraction was performed. The $(10\bar{1}0)_\epsilon$ and $(10\bar{1}1)_\epsilon$ lines decreased during heating but did not disappear completely at 250°C. A "as received" S_1 specimen was studied from room temperature (R.T.) to - 190°C, then from - 190°C \rightarrow 206°C \rightarrow R.T.

From the first experiment, the A_f point would be more than 250°C . The second experiment yields : M_s close to R.T. and A_s near 80°C (from the investigation of the $(200)_\gamma$ intensity variation). Internal friction measurements on an 1100°C as quenched specimen indicate $A_s \approx 70^\circ\text{C}$, $A_f = 100^\circ\text{C}$ and M_s close to R.T.

The electrical resistivity measurements are, after 15 thermal cycles, indicated in fig. 5. From these curves :

$$A_s = 55^\circ\text{C}, A_f = 100^\circ\text{C}, M_s = 35^\circ\text{C}$$

and, from the appearance of the antiferromagnetism of the γ phase, $T_N^\gamma = 15^\circ\text{C}$.

As already pointed out by (2) discrepancies were observed on the transition temperatures. This fact was also shown in Ni-Ti-X shape memory alloys (4). However in this study the M_f point is not obtained.

Close the M_f point, Sato et al (3) claimed an influence of the antiferromagnetism order of the γ phase. From our results, M_f is not obtained at -190°C by X ray diffraction. Magnetic susceptibility measurement were carried out between -73°C and 277°C or an as quenched alloy (fig. 6) : during cooling, we found $M_s = +8^\circ\text{C}$ whereas the Neel point of the residual austenite was $T_N^\gamma = +2^\circ\text{C}$ (the heating was stopped at room temperature). A preliminary neutron diffraction experiment showed that T_N^γ was higher than -33°C , even if other antiferromagnetic compounds were detected. Finally following magnetic and electrical measurements, we found $M_s - T_N^\gamma = +6^\circ$ or $+20^\circ\text{C}$, in agreement with the good shape recovery of the S_1 alloy. It seems to us that either the inhomogeneity of the bar, or the chemical reactivity of the alloy has to be taken in account to explain the dispersed values of the transition temperatures.

In the case of the S_2 alloy, internal friction measurements gave transition temperatures between 120°C and 360°C during heating till 400°C .

2.2. Alloys C_1 and C_2 (Fe-Mn-Cr)

In the same way, internal friction measurements on the C_1 alloy yielded transformation temperatures between 20°C and 150°C . From electrical measurements on the C_2 alloy, after one cycle, we obtained :

$$A_s \approx 50^\circ\text{C}, A_f \approx 80^\circ\text{C}, M_s \approx 60^\circ\text{C}, M_f \approx 35^\circ\text{C}.$$

Classical D.T.A. measurements failed and magnetic properties were not studied on this alloy.

DISCUSSION

For the studied alloys, the shape memory effect is the highest in the S_1 alloy but a noticeable shape memory is found in the C_2 alloy, always active four years after training. The presence of the α' phase in the S_2 alloy (may be due to the molybdenum content) and in the C_1 alloy does not prevent the phenomenon.

The structural characterization of these alloys is quite easy. The lattice parameters of the α' , γ , ϵ phases are similar. The microstructures (zig-zag martensite and stacking faults) can be explained by classical theories.

The main point of this study is the determination of the transition temperatures. Inaccurate results are obtained from electrical and internal friction measurements. X-ray diffraction experiments failed to reach A_f and M_f in the S_1 alloy. Discrepancies between X ray diffraction and physical studies in Ni-Ti-X alloys were already found, but the appearance or disappearance of phases was always detected by X ray diffraction (4).

Except the problem related to the magnetic properties in the S_1 alloy, it must be taken into account an influence of the chemical reactivity, particularly with oxygen. Before a careful electropolish, the superficial heterogeneity of the S_1 alloy is related to the appearance of the α' phase. The bar of that alloy could also contain oxygen and other reactive elements : antiferromagnetic compounds (certainly manganese oxides) are detected by neutron diffraction at 1.7 K. However, in the same temperature range repeated experiments of internal friction and electrical resistivity measurements show always variations whereas X ray diffraction lines of γ and ϵ phases are not quite modified.

Then it was thought that the development of the ϵ martensite in each sample of the S_1 alloy could be obtained by a mechanical stress (6). It is well known that the shape memory effect is related to a stress assisted transformation. On our X ray device, a "as received" sample of the S_1 alloy was stretched under the X ray beam when the $(10\bar{1}1)_\epsilon$ line became more intense. Further experiments are in progress to verify the influence of the thermal cycling at a given stress.

REFERENCES

- (1) H. OTSUKA et al., I.S.I.J. Int. 30, 9 (1990) 474
- (2) M. SADE, K. HALTER, E. HORNBOKEN, Z. Metall. K. 75, 18 (1988) 487
- (3) A. SATO, Y. YAMAJI, T. MORI, Act. Met. 34, 2 (1986) 287
- (4) V. AGAFONOV, A. DUBERTRET, G. RIZZO, B. DUBOIS, I.C.O.M.A.T. 89, Mat. Sci. Forum 56-58 (1990) 625
- (5) A. SATO, Proceedings of the M.R.S., Vol. 9 (1988) 431
- (6) B. DUBOIS, Traitement thermique, 234 (1990) 27.

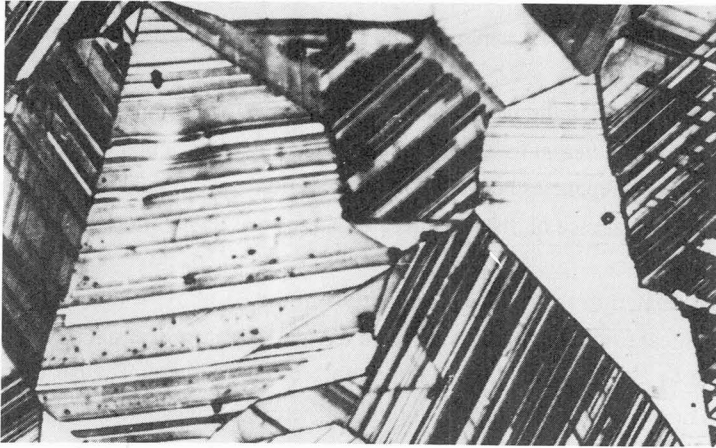


Figure 1 : Optical micrograph of as received S1 alloy (x 250).



Figure 2 : Stacking faults in as quenched S1 alloy (x 30.000).

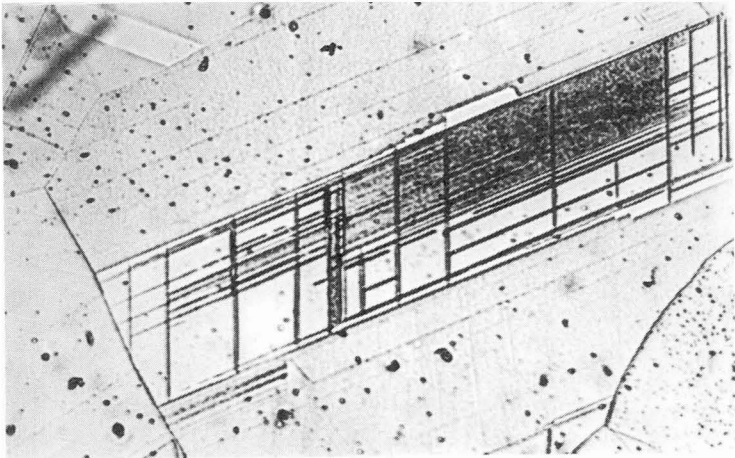


Figure 3 : Optical micrograph of as quenched C2 alloy (x 400).

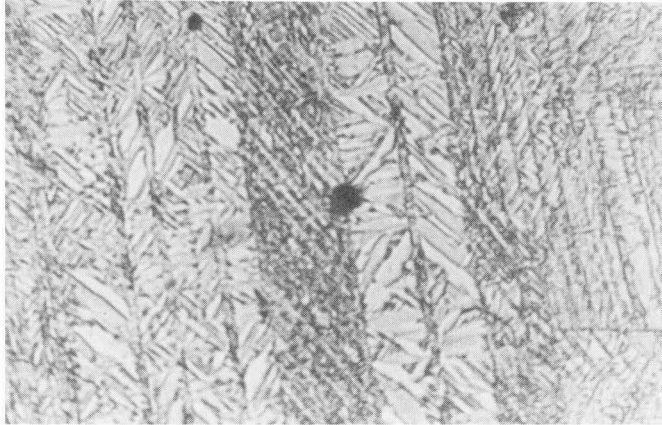


Figure 4 : Optical micrograph of as quenched C1 alloy (x 250).

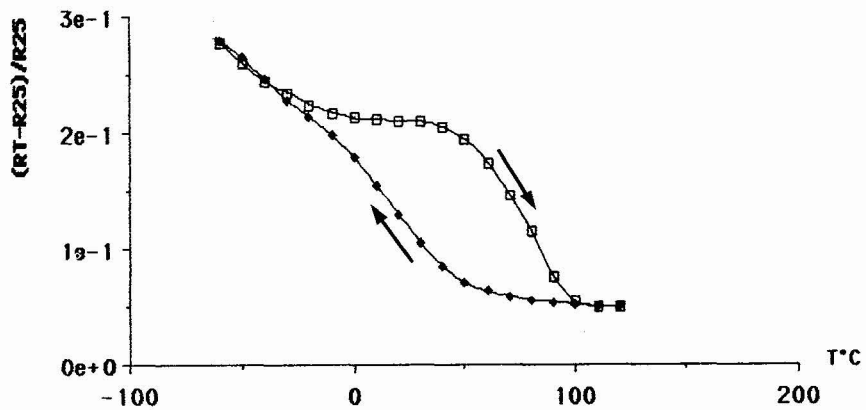


Figure 5 : Resistivity measurements of as received S1 alloy after 15 thermal cycles.

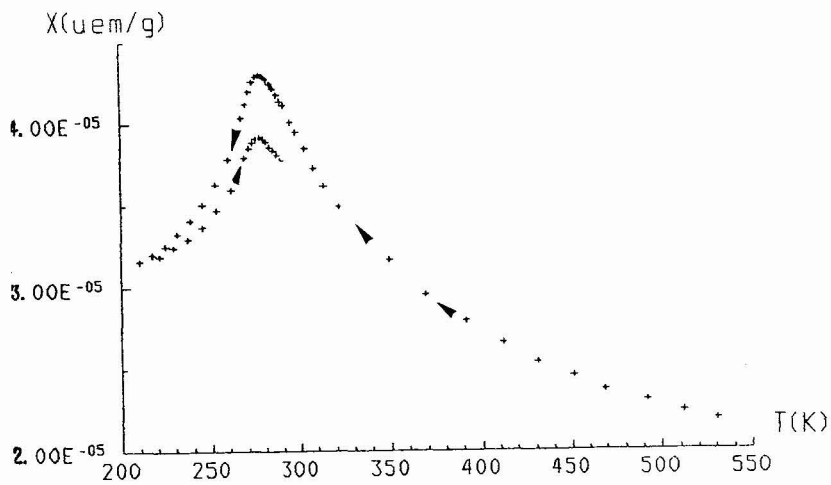


Figure 6 : Magnetic susceptibility of as quenched S1 alloy.